

A local void and the accelerating Universe

K. Tomita[★]

Yukawa Institute for Theoretical Physics, Kyoto University, Kyoto, 606-8502, Japan

Accepted 2001 April 12. Received 2001 April 12; in original form 2000 December 1

ABSTRACT

Corresponding to the recent observational claims that we are in a local void (an underdense region) on scales of 200–300 Mpc, the magnitude–redshift relation in a cosmological model with a local void is investigated. It is already evident that the accelerating behaviour of high- z supernovae can be explained in this model, because the local void plays a role similar to the positive cosmological constant. In this paper the dependence of the behaviour on the gaps of cosmological parameters in the inner (low-density) region and the outer (high-density) region, the radius of the local void, and the clumpiness parameter is studied and its implications are discussed.

Key words: cosmology: observations – large-scale structure of Universe.

1 INTRODUCTION

One of the most important cosmological observations at present is the $[m, z]$ relation for high- z supernovae (SNIa), which act as standard candles at the stage reaching epochs $z \gtrsim 1$. So far the observed data of SNIa have been compared with the theoretical relation in homogeneous and isotropic models, and many workers have made efforts to determine their model parameters (Garnavich et al. 1998; Schmidt et al. 1998; Perlmutter et al. 1999; Riess et al. 1998, 2000; Riess 2000).

There is, however, an essentially important problem to be taken into consideration: the homogeneity of the Universe. According to Giovanelli et al. (1998, 1999) and Dale et al. (1999), the Universe is homogeneous in the region within $70 h^{-1}$ Mpc (the Hubble constant H_0 is $100 h \text{ km s}^{-1} \text{ Mpc}^{-1}$). On the other hand, recent galactic redshift surveys (Marinoni et al. 1999; Marzke et al. 1998; Folkes et al. 1999; Zucca et al. 1997) show that in the region around 200–300 h^{-1} Mpc from us, the distribution of galaxies may be inhomogeneous. This is because the galactic number density in the region of $z < 0.1$ or $< 300 h^{-1}$ Mpc from us was shown to be smaller by a factor of > 1.5 than that in the remote region of $z > 0.1$. Recently a large-scale inhomogeneity suggesting a wall around the void on scales of $\sim 250 h^{-1}$ Mpc has been found by Blanton et al. (2001) in the SDSS commissioning data (cf. their figs 7 and 8). Similar walls on scales of $\sim 250 h^{-1}$ Mpc have already been found in the Las Campanas and 2dF redshift surveys near the northern and southern Galactic caps (Shectman et al. 1996; Folkes et al. 1999; Cole et al. 2001). These results mean that there is a local void with a radius of 200–300 h^{-1} Mpc and we live in it.

Moreover, the measurements by Hudson et al. (1999) and Willick (1999) for a systematic deviation of the motions of clusters from the global Hubble flow may show some inhomogeneity on

scales larger than $100 h^{-1}$ Mpc. Another suggestion for inhomogeneity comes from the periodic wall structures on scales of $\sim 130 h^{-1}$ Mpc, as have been shown by Broadhurst et al. (1990), Landy et al. (1996) and Einasto et al. (1997). This is connected with the anomaly of the power spectrum around $100\text{--}200 h^{-1}$ Mpc (so-called ‘excess power’) which was discussed by Einasto et al. (1999). This fact also may suggest some inhomogeneity in the above nearby region.

If the local void really exists, the Hubble constant must also be inhomogeneous, as must the density parameters, and the theoretical relations between observed quantities are different from those in homogeneous models. At present, however, the large-scale inhomogeneity of the Hubble constant has not yet been observationally established because of the large error bars in the various measurements (cf. Tomita 2001).

In my previous papers (Tomita 2000a,b), cited as Paper I and Paper II, I showed various models with a local void and discussed the bulk flow, cosmic microwave background (CMB) dipole anisotropy, distances and the $[m, z]$ relation in them in the limited parameter range. It was found that the accelerating behaviour of supernovae can be explained in these models without a cosmological constant. On the other hand, Kim et al. (1997) showed that the difference between the local and global values of the Hubble constant should be smaller than 10 per cent in *homogeneous* cosmological models in order to be consistent with the SNIa data. However, this does not impose any strong condition on the difference in inhomogeneous models, because their analyses were done using the luminosity distance in *homogeneous* models and so they are incomplete. In fact my previous papers showed concretely that, in inhomogeneous models, larger differences can be consistent with the data. The possibility that the above difference may explain the behaviour of SNIa was later discussed also by Goodwin et al. (1999).

In this paper I describe first (in Section 2) a simplified

[★]E-mail: tomita@yukawa.kyoto-u.ac.jp

cosmological model with a local void, and treat distances in light paths with the non-zero clumpiness (smoothness) parameter α . In the previous paper (Paper II), I considered only distances in full-beam light paths ($\alpha = 1$), but in realistic paths there are deviations from $\alpha = 1$ as a result of lensing effects from inhomogeneous matter distributions. In Section 3, I show the dependence of the $[m, z]$ relation on model parameters such as the radius of the local void, the ratios of density parameters and Hubble constants in the inner (low-density) and outer (high-density) regions, and the clumpiness parameter. The constraints to the parameters are derived in comparison between the above relations in the present models and the relations in homogeneous models.

Finally, in Section 4, we discuss the remaining problems and describe concluding remarks.

2 DISTANCES IN MODELS WITH A LOCAL VOID

The inhomogeneous models we consider consist of an inner (low-density) region V^I and an outer (high-density) region V^{II} , which are separated by a single shell. It is treated as a spherical singular shell and the mass in it compensates for the mass deficiency in V^I . So V^I and the shell are regarded as a local void and the wall, respectively. The line-elements in the two regions are

$$ds^2 = g_{\mu\nu}^j(dx^j)^\mu(dx^j)^\nu = -c^2(dt^j)^2 + [a^j(t^j)]^2 \{d(\chi^j)^2 + [f^j(\chi^j)]^2 d\Omega^2\}, \quad (1)$$

where j ($=I$ or II) represents the regions, $f^j(\chi^j) = \sin \chi^j$, χ^j and $\sinh \chi^j$ for $k^j = 1, 0, -1$, respectively, and $d\Omega^2 = d\theta^2 + \sin^2\theta d\varphi^2$. In the following, the negative curvature is assumed in all regions. The Hubble constants and density parameters are expressed as (H_0^I, H_0^{II}) and $(\Omega_0^I, \Omega_0^{II})$, where we assume that $H_0^I > H_0^{II}$ and $\Omega_0^I < \Omega_0^{II}$. The distances of the shell and the observer O (in V^I) from the centre C (in V^I) are assumed to be 200 and $40 h_1^{-1}$ as a standard case. This shell corresponds to the redshift $\bar{z}_1 = 0.067$ (see Fig. 1).

In Paper II we derived the full-beam distances (\overline{CS}) between the centre C and a source S , and the distances (\overline{OS}) between an observer O and S . The two distances are nearly equal in the case

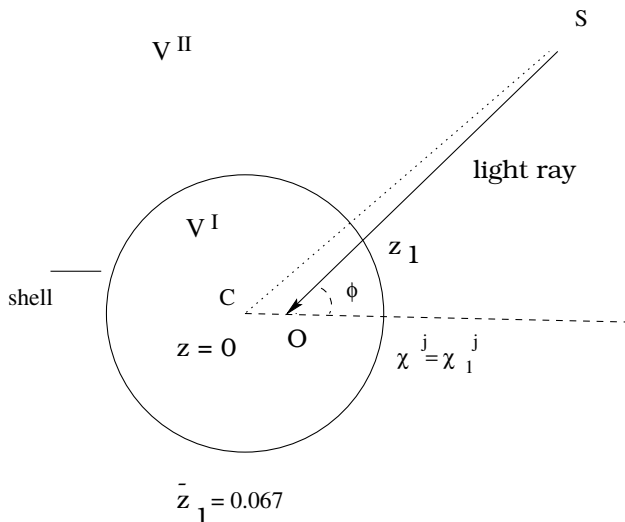


Figure 1. Model with a spherical single shell. Redshifts for observers at O and C are z and \bar{z} .

when \overline{CS} or \overline{OS} is much larger than \overline{CO} . Since this is the only case we deal with in the following, we treat the light paths as being \overline{CS} for simplicity. Then the angular-diameter distance d_A is

$$d_A = a^I(\bar{\eta}_s^I) \sinh(\bar{\chi}_s^I), \quad (2)$$

if a source S is in V^I , where $(\bar{\eta}_s^I, \bar{\chi}_s^I)$ are the coordinates of S , and η is the conformal time coordinate. Here bars are used for the coordinates along the light paths to the virtual observer at C . If S is in V^{II} , we have

$$d_A = a^I(\bar{\eta}_1^I) \sinh(\bar{\chi}_1^I) + [a^{II}(\bar{\eta}_s^{II}) \sinh(\bar{\chi}_s^{II}) - a^{II}(\bar{\eta}_1^{II}) \sinh(\bar{\chi}_1^{II})], \quad (3)$$

where $(\bar{\eta}_1^I, \bar{\chi}_1^I)$ stand for the shell, and we have

$$a^I(\bar{\eta}_1^I) \sinh(\bar{\chi}_1^I) = a^{II}(\bar{\eta}_1^{II}) \sinh(\bar{\chi}_1^{II}) \quad (4)$$

from the junction condition.

Here we treat the following equation for the angular-diameter distance to take into consideration the clumpiness along the paths (Dyer & Roeder 1973; Schneider, Ehler & Falco 1992; Kantowski 1998; Tomita 1999):

$$\frac{d^2(d_A^j)}{d(z^j)^2} + \left\{ \frac{2}{1+z^j} + \frac{1}{2}(1+z^j)[\Omega_0^j(1+3z^j) + 2 - 2\chi_0^j]F^{-1} \right\} \times \frac{d(d_A^j)}{dz^j} + \frac{3}{2}\Omega_0^j\alpha(1+z^j)F^{-1}d_A^j = 0, \quad (5)$$

where $j = I$ and II , z^j is the redshift in the region V^j , α is the clumpiness parameter, and

$$F \equiv (1 + \Omega_0^j z^j)(1 + z^j)^2 - \chi_0^j z^j (2 + z^j). \quad (6)$$

Here and in the following the bars are omitted for simplicity. The two redshifts at the shell are equal, i.e.

$$z_1^I = z_1^{II} \quad (\equiv z_1) \quad (7)$$

for the comoving shell (cf. Paper I).

The distances d_A^I in V^I is obtained solving equation (5) under the conditions at $z^I = 0$:

$$(d_A^I)_0 = 0, \quad (d_A^I/dz^I)_0 = c/H_0^I, \quad (8)$$

and d_A^{II} in V^{II} is obtained similarly under the conditions at $z^{II} = 0$:

$$(d_A^{II})_0 = \text{constant}, \quad (d_A^{II}/dz^{II})_0 = c/H_0^{II}, \quad (9)$$

where constant is determined so that the junction condition $d_A^I(z_1) = d_A^{II}(z_1)$ may be satisfied at the shell. Then the distance $d_A(z_s)$ from C to the source S is

$$d_A(z_s) = d_A^I(z_s) \quad \text{for } z_s \leq z_1, \quad (10)$$

and

$$d_A(z_s) = d_A^I(z_1) + d_A^{II}(z_s) - d_A^{II}(z_1) \quad \text{for } z_s > z_1, \quad (11)$$

where $z_s = z_s^I$ and z_s^{II} for $z_s \leq z_1$ and $z_s > z_1$, respectively. The luminosity distance d_L is related to the angular-diameter distance d_A by $d_L = (1+z)^2 d_A$.

As for the clumpiness parameter α , we studied the distribution function $N(\alpha)$ as a function of z in our previous papers (Tomita 1998, 1999). To obtain $N(\alpha)$, we first derived model universes consisting of galaxies and haloes using an N -body simulation technique; secondly, we calculated the angular-diameter distance by solving null-geodesic equations along many light paths between an observer and sources at epoch z , and finally we derived a

statistical distribution of α determined in a comparison with the Friedmann distance ($\alpha = 1.0$) and the Dyer–Roeder distance ($\alpha = 0.0$). As the result of these studies, it was found that the average value $\bar{\alpha}$ of α is 1.0, which represents the Friedmann distance, and the dispersion σ_α can be ~ 0.5 for $z < 2.0$. If the detection of high- z supernovae is done in completely random directions, the observed average value of α is equal to the above theoretical average value $\bar{\alpha}$. However, if the detections are biased to the directions with a lower galactic number per steradian to avoid the dust obscuration, we may have the value of $\alpha \sim \bar{\alpha} - \sigma_\alpha$. Then the angular-diameter and luminosity distances are somewhat longer than the average Friedmann distances. In the next section, we show the cases with $\alpha = 1.0, 0.5$, and 0.0 for comparison. The lensing effect on the $[m, z]$ relation of SNIa has also been discussed by Holz (1998), Porciani & Madau (2000) and Barber (2000).

3 PARAMETER DEPENDENCE OF THE MAGNITUDE-REDSHIFT RELATION

As for homogeneous models, it is well-known from the comparison

with observational data that the flat case with non-zero cosmological constant of $(\Omega_0, \lambda_0) = (0.3, 0.7)$ can represent the accelerating behaviour of high- z SNIa, while an open model with $(0.3, 0)$ cannot explain their data for $z \approx 1.0$ (Garnavich et al. 1998; Schmidt et al. 1998; Perlmutter et al. 1999; Riess et al. 1998, 2000; Riess 2000). In the present inhomogeneous models, we have six model parameters $(\Omega_0^I, \lambda_0^I, H_0^I, H_0^{II}/H_0^I, \Omega_0^{II}/\Omega_0^I, z_1)$, and their direct fitting with the observational data is very complicated in contrast to the homogeneous case, which has three parameters. In this paper, the parameter dependence of $[m, z]$ relations is examined for the preliminary study, and the relations in these two homogeneous models are used as a measure for inferring how the relations in inhomogeneous models with various parameters can reproduce the observational data. That is, we deduce that the model parameters are consistent with the observational data, if at the interval $0.5 < z < 1.0$ the curve in the $[m, z]$ relation is similar to that in the homogeneous model $(0.3, 0.7)$ comparing with the difference between the curves for $(0.3, 0.7)$ and $(0.3, 0)$.

For the $[m, z]$ relation in an inhomogeneous model, we first treat the case with the following *standard* parameters to reproduce the accelerating behaviour in the above homogeneous model $(0.3, 0.7)$

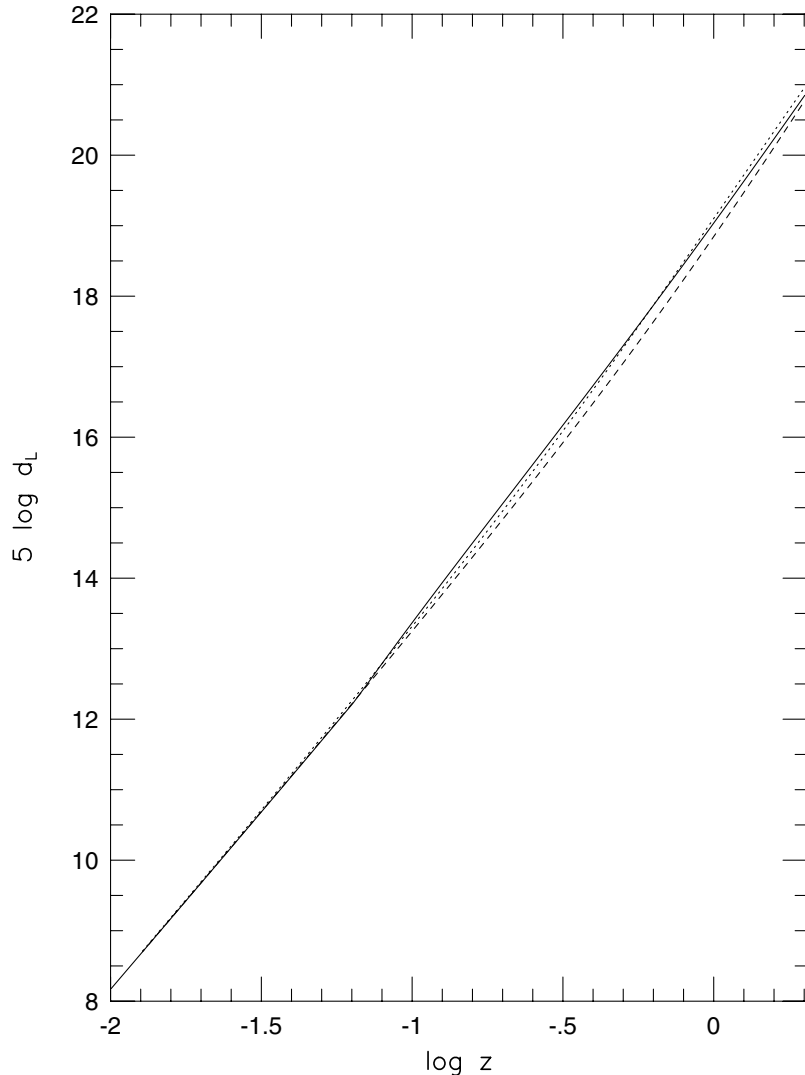


Figure 2. The $[m, z]$ relation in cosmological models with a local void. The solid line denotes the case with a standard parameter set given in equation (12). The dotted and dashed lines stand for homogeneous models with $(\Omega_0, \lambda_0) = (0.3, 0.7)$ and $(0.3, 0.0)$, respectively, for comparison.

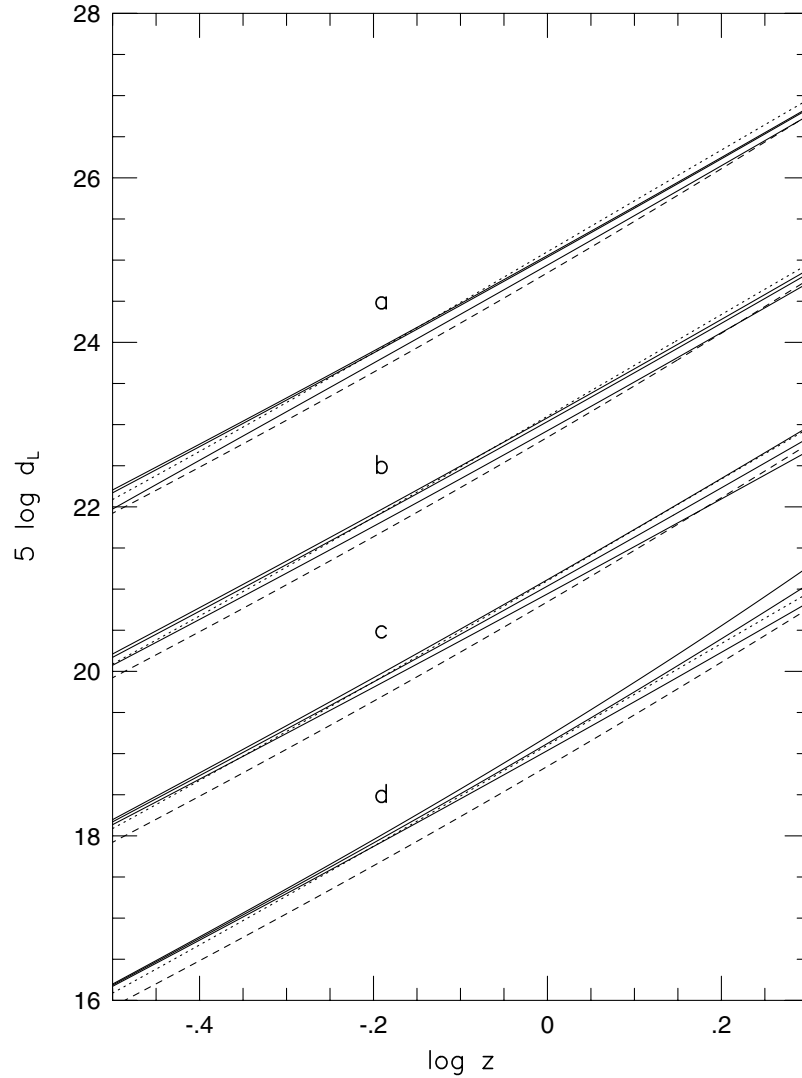


Figure 3. The $[m, z]$ relation in cosmological models with a local void. The solid lines denote: (a) the cases with $z_1 = 0.05, 0.067$, and 0.167 (from the top to the bottom), which correspond to the shell radius $r_1 = 150, 200$, and $500(h_1)^{-1}$ Mpc, respectively; (b) the cases with $H_0^{\text{II}}/H_0^{\text{I}} = 0.87, 0.82$, and 0.80 from the top to the bottom; (c) the cases with $\Omega_0^{\text{II}} = 0.45, 0.6$, and 0.8 from the top to the bottom; and (d) the cases with $\alpha = 0.0, 0.5$, and 1.0 from the top to the bottom. The other parameters are the same as those in a standard parameter set given in (12). The dotted and dashed lines stand for homogeneous models, as in Fig. 2. Curves (a), (b) and (c) were depicted in the single figure together with (d) by shifting upward as $\Delta(5 \log d_L) = 6, 4, 2$, respectively.

in a similar way.

$$(\Omega_0^{\text{I}}, \Omega_0^{\text{II}}) = (0.3, 0.6),$$

$$H_0^{\text{I}} = 71, \quad H_0^{\text{II}}/H_0^{\text{I}} = 0.82,$$

$$\alpha = 1.0, \quad z_1 = 0.067, \quad \text{and} \quad \lambda_0^{\text{I}} = \lambda_0^{\text{II}} = 0. \quad (12)$$

The radius of the local void is $r_1 \equiv (c/H_0^{\text{I}})z_1 = 200(h_1)^{-1}$ Mpc. In Fig. 2, the relation is shown for $z = 0.01$ – 2.0 in comparison with that in two homogeneous models with parameters: $(\Omega_0, \lambda_0) = (0.3, 0.7)$ and $(0.3, 0)$, $H_0 = 71$ and $\alpha = 1.0$. For $z < z_1$ the relation is equal to that in the open model $(0.3, 0.0)$.

It is found that the behaviour in the case of $(\Omega_0^{\text{I}}, \Omega_0^{\text{II}}) = (0.3, 0.6)$ with $\lambda_0^{\text{I}} = \lambda_0^{\text{II}} = 0$ accords approximately with that in the flat, homogeneous model with $(\Omega_0, \lambda_0) = (0.3, 0.7)$ for $z_1 < z < 1.0$. Accordingly there is a similar fit for the observed data of SNIa.

Next, to examine the parameter dependence of the $[m, z]$ relation, we take up various cases with the following parameters

(different from the above standard case):

$$\Omega_0^{\text{II}} = 0.45 \text{ and } 0.80 \quad (\text{for } \Omega_0^{\text{I}} = 0.3)$$

$$H_0^{\text{II}}/H_0^{\text{I}} = 0.80 \text{ and } 0.87 \quad (\text{for } H_0^{\text{I}} = 71),$$

$$\alpha = 0.0 \text{ and } 0.5, \quad z_1 = 0.05 \text{ and } 0.167, \quad \text{and}$$

$$\lambda_0^{\text{II}} = 0.4. \quad (13)$$

Here, for $z_1 = 0.05$ and 0.167 , we have $r_1 = (150 \text{ and } 500)(h_1)^{-1}$ Mpc, respectively. Since $\lambda_0^{\text{I}} \equiv \frac{1}{3}\Lambda(c/H_0^{\text{I}})^2$, we have $\lambda_0^{\text{I}} = \lambda_0^{\text{II}}(H_0^{\text{II}}/H_0^{\text{I}})^2$.

In Fig. 3 (curves a), the cases with $z_1 = 0.05, 0.067$ and 0.167 are shown in a model with $(\Omega_0^{\text{I}}, \Omega_0^{\text{II}}) = (0.3, 0.6)$, $H_0^{\text{II}}/H_0^{\text{I}} = 0.82$, $\alpha = 1.0$, and $\lambda_0^{\text{I}} = \lambda_0^{\text{II}} = 0$. The range of z was changed to $0.3 < z < 2.0$ to magnify the figures. From this figure it may be seen that if $r_1 = 150$ and $200(h_1)^{-1}$ Mpc, the $[m, z]$ relation is similar to that in the flat, homogeneous model with $(\Omega_0, \lambda_0) = (0.3, 0.7)$ for $z \sim 0.5$, but if $r_1 = 500(h_1)^{-1}$ Mpc, the relation is rather different

from that in the latter model. This means that r_1 must be $\leq 300(h_1)^{-1}$ Mpc to explain the $[m, z]$ relation of SNIa. This observational constraint is consistent with the observationally estimated radius of the local void ($\leq 300 h^{-1}$ Mpc) (cf. Marinoni et al. 1999; Marzke et al. 1998; Folkes et al. 1999; Zucca et al. 1997).

In Fig. 3 (curves b), the cases with $H_0^{\text{II}}/H_0^{\text{I}} = 0.80, 0.82,$ and 0.87 are shown in a model with $(\Omega_0^{\text{I}}, \Omega_0^{\text{II}}) = (0.3, 0.6)$, $z_1 = 0.067$, $\alpha = 1.0$, and $\lambda_0^{\text{I}} = \lambda_0^{\text{II}} = 0$. In the cases with $H_0^{\text{II}}/H_0^{\text{I}} = 0.82, 0.87$, the relations are found to be consistent with the relation in the above flat, homogeneous model for $z = 0.5-1.0$, but in the case with $H_0^{\text{II}}/H_0^{\text{I}} = 0.80$ or < 0.80 , the $[m, z]$ relation is difficult to explain the observed data.

In Fig. 3 (curves c), the cases with $\Omega_0^{\text{II}} = 0.45, 0.6,$ and 0.8 are shown in a model with $\Omega_0^{\text{I}} = 0.3$, $H_0^{\text{II}}/H_0^{\text{I}} = 0.82$, $z_1 = 0.067$, $\alpha = 1.0$, and $\lambda_0^{\text{I}} = \lambda_0^{\text{II}} = 0$. In the case with $\Omega_0^{\text{II}} = 0.45$ and 0.6 , the relations are found to be consistent with those in the above flat,

homogeneous model for $z = 0.5-1.0$, but in the case with $\Omega_0^{\text{II}} = 0.8$ we have less consistency.

Here let us examine the lensing effect on the $[m, z]$ relation. In Fig. 3 (curves d), the cases with $\alpha = 0.0, 0.5,$ and 1.0 are shown in a model with $(\Omega_0^{\text{I}}, \Omega_0^{\text{II}}) = (0.3, 0.6)$, $H_0^{\text{II}}/H_0^{\text{I}} = 0.82$, $z_1 = 0.067$, and $\lambda_0^{\text{I}} = \lambda_0^{\text{II}} = 0$. Compared with the case $\alpha = 1.0$, the relations for $\alpha = 0.0$ and 0.5 , give larger magnitudes especially at epochs $z > 1.0$. For $\alpha = 0.5$, the magnitudes are larger by about 0.1 and 0.2 mag than those for $\alpha = 1.0$ in the relations at epochs $z = 1.0$ and 2.0 , respectively. If the value $\alpha = 0.5$ is realistic, the cases with larger Ω_0^{II} and smaller $H_0^{\text{II}}/H_0^{\text{I}}$ may be consistent with the observed data.

Next we consider the cases with a non-zero cosmological constant. In Fig. 4 (curves a), the cases with $\lambda_0^{\text{II}} = 0.0$ and 0.4 are shown in a model with $(\Omega_0^{\text{I}}, \Omega_0^{\text{II}}) = (0.3, 0.6)$, $H_0^{\text{II}}/H_0^{\text{I}} = 0.82$, $z_1 = 0.067$, and $\alpha = 1.0$. In the case with $\lambda_0^{\text{II}} = 0.4$, the space in the outer region is spatially flat. In this case, the role of the

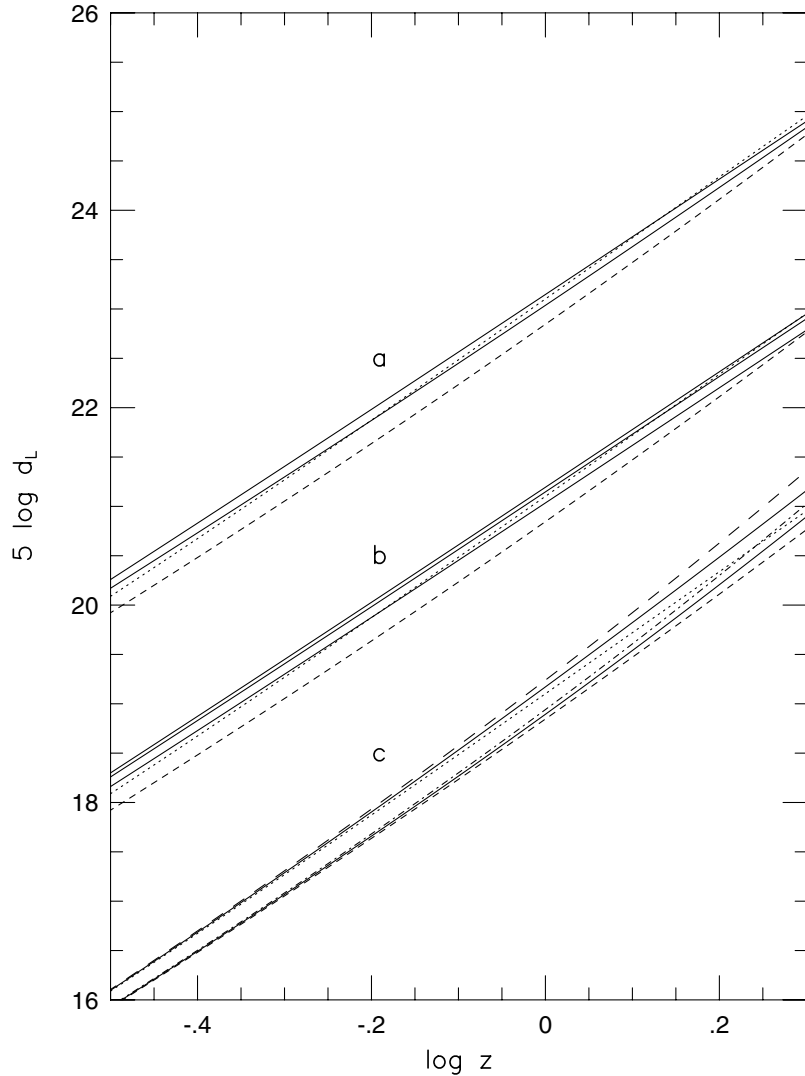


Figure 4. The $[m, z]$ relation in cosmological models with a local void. The upper and lower solid lines denote: (a) the cases with $\lambda_0^{\text{II}} = 0.4$ and 0.0 , respectively; and (b) the cases with $H_0^{\text{II}}/H_0^{\text{I}} = 0.87, 0.82,$ and 0.80 for $\lambda_0^{\text{II}} = 0.4$ from the top to the bottom. (c) The $[m, z]$ relation in two homogeneous cosmological models with $(\Omega_0, \lambda_0) = (0.3, 0.7)$ and $(0.3, 0.0)$. The upper and lower groups of three lines stand for models $(0.3, 0.7)$ and $(0.3, 0.0)$. The upper, middle and lower lines in each group are for $\alpha = 0.0, 0.5,$ and 1.0 , respectively. The other parameters are same as those in a standard parameter set given in (12). The dotted and dashed lines stand for homogeneous models, as in Fig. 2. Curves (a) and (b) were depicted in the single figure together with (c) by shifting upward as $\Delta(5 \log d_L) = 4, 2,$ respectively.

cosmological constant to the accelerating behaviour is not dominant, but is supplementary to the role of the local void.

In Fig. 4 (curves b), the cases with $H_0^{\text{II}}/H_0^{\text{I}} = 0.80, 0.82,$ and 0.87 are shown in a model with $(\Omega_0^{\text{I}}, \Omega_0^{\text{II}}) = (0.3, 0.6), z_1 = 0.067,$ $\alpha = 1.0,$ and $\lambda_0^{\text{II}} = 0.4.$ In this outer-flat case also, larger $H_0^{\text{II}}/H_0^{\text{I}}$ gives larger magnitudes in the $[m, z]$ relation.

Finally, the lensing effect in homogeneous models is examined for comparison. In Fig. 4 (curves c), the cases with $\alpha = 0.0, 0.5,$ and 1.0 are shown in homogeneous models with $(\Omega_0, \lambda_0) = (0.3, 0.7)$ and $(0.3, 0)$ for $H_0 = 71.$ As in Fig. 3 (set of curves d), the magnitudes in the relation for $\alpha = 0.5$ are larger by about 0.1 and 0.2 mag than those for $\alpha = 1.0$ in the relations at epochs $z = 1.0$ and $2.0,$ respectively.

4 CONCLUDING REMARKS

As for the $[m, z]$ relation in cosmological models with a local void, we studied the parameter dependence of their accelerating behaviour, and found that the local void with $r_1 \leq 200 h^{-1}$ Mpc, $H_0^{\text{II}}/H_0^{\text{I}} \geq 0.82,$ and $\Omega_0^{\text{II}} \leq 0.6$ is appropriate for explaining the accelerating behaviour of SNIa without a cosmological constant, that the lensing with $\alpha \sim 0.5$ is effective at epochs of $z \geq 1.0,$ and that the cosmological constant ($\lambda_0^{\text{II}} \sim 0.4$) necessary for flatness in the outer region has a role supplementary to the accelerating behaviour. On the basis of these results, the next step is determining what values of the model parameters are best for a direct comparison with the observational data of SNIa.

In the Universe with cold dark matter, the probability that the inhomogeneity of Hubble constant $\delta H/H \sim 0.2$ on scales ~ 200 Mpc associated with general density perturbations is realized is extremely small, as was clarified and discussed by Turner, Cen & Ostriker (1992), Nakamura & Suto (1995), Shi & Turner (1998) and Wang, Spergel & Turner (1998). The constraint from CMB dipole anisotropy was also discussed by Wang et al. (1998). It should be noticed here that the *spherical* void which we are considering is exceptionally compatible with the constraint from CMB dipole anisotropy, in spite of the above large deviation of the Hubble constant, as long as the observers are near the centre (cf. Paper I). Inversely, it may be suggested that the local void on scales ~ 200 Mpc must be *spherical* or *nearly spherical*, if its existence is real.

In comparison with observations of the galactic number count–magnitude relation, on the other hand, Phillips & Turner (1998) have once studied the possibility of an underdense region on scales of $\sim 300 h^{-1}$ Mpc. However, a necessary wall for the mass compensation has not been considered in their simple models and, in the small-angle observations of the above relation, the boundary between the inside region and the outside region was rather vague in contrast to the large-angle redshift surveys.

In the near future the void structure on scales of $\sim 200 h^{-1}$ Mpc will be clarified by the galactic redshift survey of SDSS in the dominant part of whole sky. Then, observational cosmology will be developed, taking into account the fact that we are in a local void.

ACKNOWLEDGMENTS

The author thanks K. Shimasaku for discussions on galactic

redshift surveys and V. Müller for helpful comments. This work was supported by Grant-in Aid for Scientific Research (No. 12440063) from the Ministry of Education, Science, Sports and Culture, Japan.

REFERENCES

- Barber A. J., 2000, MNRAS, 318, 195
 Blanton, 2001, AJ, 121, 2358
 Broadhurst T. J., Ellis R. S., Koo D. C., Szalay A. S., 1990, Nat, 343, 726
 Cole S., Norberg P., Baugh C. M., Frenk C. S., Bland-Hawthorn J., Bridges T., Cannon R., Colless M., 2001, MNRAS, in press (astro-ph/0012429)
 Dale D. A., Giovanelli R., Haynes M. P., Hardy E., Campusano L., 1999, ApJ, 510, L11
 Dyer C. C., Roeder R. C., 1973, ApJ, 180, L31
 Einasto J. et al., 1997, Nat, 385, 139
 Einasto J., Einasto M., Tago E., Starobinsky A. A., Atrio-Barandela F., Müller V., Knebe A., Cen R., 1999, ApJ, 519, 469
 Folkes S. et al., 1999, MNRAS, 308, 459
 Garnavich P. M. et al., 1998, ApJ, 493, L53
 Giovanelli R., Haynes M. P., Freudling W., da Costa L., Salzer J., Wegner G., 1998, ApJ, 505, L91
 Giovanelli R., Dale D. A., Haynes M. P., Hardy E., Campusano L., 1999, ApJ, 525, 25
 Goodwin S. P., Thomas P. A., Barber A. J., Gribbin J., Onuora L. I., 1999, astro-ph/9906187 (unpublished)
 Holz D. E., 1998, ApJ, 506, L1
 Hudson M. J., Smith R. J., Lucey J. R., Schlegel D. J., Davies R. L., 1999, ApJ, 512, L79
 Kantowski R., 1998, ApJ, 507, 483
 Kim A. G. et al., 1997, ApJ, 476, L63
 Landy S. D., Shectman S. A., Lin H., Kirshner R. P., Oemler A. A., Tucker D., 1996, ApJ, 456, L1
 Marinoni C., Monaco P., Giuricin G., Costantini B., 1999, ApJ, 521, 50
 Marzke R. O., da Costa L. N., Pellegrini P. S., Willmer C. N. A., Geller M. J., 1998, ApJ, 503, 617
 Nakamura T. T., Suto Y., 1995, ApJ, 447, L65
 Perlmutter S. et al., 1999, ApJ, 517, 565
 Phillips L. A., Turner E. L., 1998, astro-ph/9802352 (unpublished)
 Porciani C., Madau P., 2000, ApJ, 532, 679
 Riess A. G. et al., 1998, AJ, 116, 1009
 Riess A. G., Filippenko A. V., Li W., Schmidt B., 2000, AJ, 118, 2668
 Riess A. G., 2000, PASP, 112, 1284
 Shectman S. A., Landy S. D., Oemler A., Tucker D. L., Lin H., Kirshner R. P., Schechter P. L., 1996, ApJ, 470, 172
 Schmidt B. P. et al., 1998, ApJ, 507, 46
 Schneider P., Ehler J., Falco E. E., 1992, Gravitational Lenses. Springer, Berlin
 Shi X., Turner M. S., 1998, ApJ, 493, 519
 Tomita K., 1998, Prog. Theor. Phys., 100, 79
 Tomita K., 1999, Prog. Theor. Phys. Suppl., 133, 155
 Tomita K., 2000a, ApJ, 529, 26 (Paper I)
 Tomita K., 2000b, ApJ, 529, 38 (Paper II)
 Tomita K., 2001, Prog. Theor. Phys., 105, 419
 Turner E. L., Cen R., Ostriker J. P., 1992, AJ, 103, 1427
 Wang Y., Spergel D. S., Turner E. L., 1998, ApJ, 489, 1
 Willick J. A., 1999, ApJ, 522, 647
 Zucca E. et al., 1997, A&A, 326, 477

This paper has been typeset from a $\text{\TeX}/\text{\LaTeX}$ file prepared by the author.